

# CONTENTS

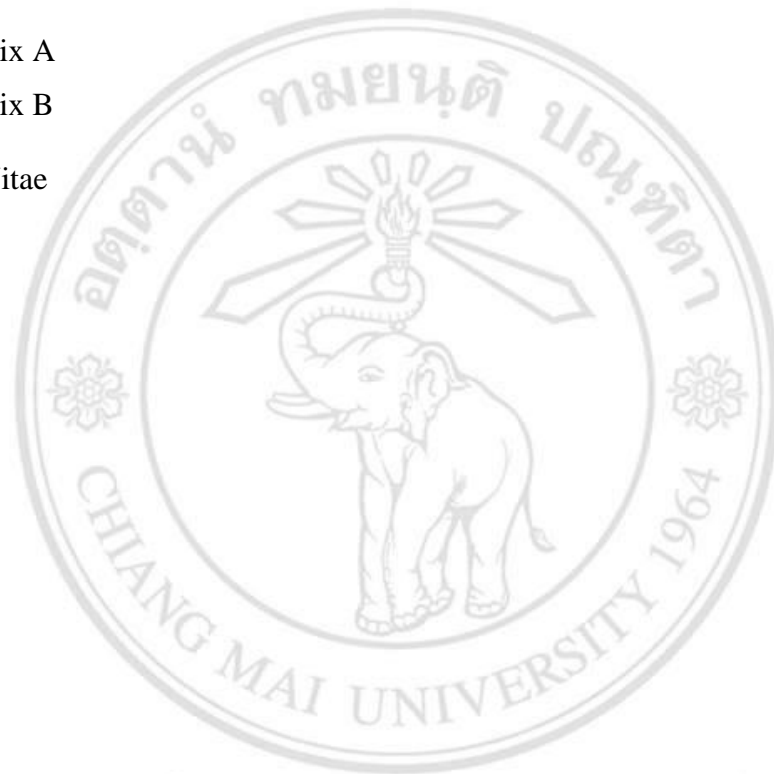
	Page
Acknowledgement	d
Abstract in Thai	f
Abstract in English	i
List of Tables	q
List of Figures	s
List of Abbreviations	cc
List of Symbols	ff
Statement of Originality in Thai	gg
Statement of Originality in English	hh
Chapter 1 Introduction	1
1.1. Introduction to ferroelectric glass-ceramics	1
1.2. Objective	5
1.3. Usefulness of the Research	5
Chapter 2 Theory and Literature Review	6
2.1. Ferroelectric Property for Glass-ceramics	6
2.1.1. Ferroelectric Characteristics	7
2.1.2. Perovskite Type Structure	11
2.1.3. Potassium Sodium Niobate	14
2.2. Glass-Ceramics	21
2.2.1. Theory of Glass and Glass-ceramics	24
2.2.2. Hypothesis of Crystallization in Glass-ceramic	29

2.2.3. Transparent Ferroelectric Glass-Ceramics (TFCGs)	32
2.2.4. Material System	33
1) Tellurite glass	35
2) Silicate glass	36
2.3. Rare Earth Doped Material	37
2.3.1. The Study of Er <sub>2</sub> O <sub>3</sub> Dopant to TeO <sub>2</sub> Glass System	41
2.3.2. The Study of Er <sub>2</sub> O <sub>3</sub> Dopant Effect to Ceramics System	44
2.3.3. The Study of Er <sub>2</sub> O <sub>3</sub> Dopant Effect to Silicate Glass System	47
Chapter 3 Experimental Procedure	50
3.1. Chemical Reagents and Laboratory Instruments	51
3.1.1. Chemical Reagent Lists	51
3.1.2. Laboratory Instruments	52
3.2. Sample Preparation	52
3.2.1. Powder Preparation	52
3.2.2. Glass Preparation	56
3.2.3. Crystallization Process	58
3.3. Glass-ceramics Characterization	59
3.3.1. Thermal Analysis	59
3.3.2. Densification Analysis	61
3.3.3. Phase Analysis	62
1) X-ray Diffractometer	62
2) Raman Spectroscopy	62
3) FTIR spectroscopy operating system	63
3.3.4. Microstructure Analysis	64
3.3.5. Measurement of Optical Properties	65
1) Transmittance (%) and Absorbance	65
2) Refractive Index	67
2.1) Reflectometry	68
2.2) Ellipsometry	68
2.3) Photoluminescence	70
3.3.6. Electrical Measurement	72

Chapter 4 Results and Discussion (Part I)	74
Materials Characterization of Potassium Sodium Niobate Based Tellurite Glass and Glass-ceramic	
4.1. The Characterization Of KNN-TeO <sub>2</sub> Glass and Glass-Ceramics	74
4.1.1. Thermal Behavior Determination	76
4.1.2. Densification Investigation	79
4.1.3. Structural Formation	80
1) Phase Composition Studied By XRD	80
2) Phase Formation Studied By FTIR	83
4.1.4. Microstructure Observation	84
4.1.5. Electrical Property	88
1) Dielectric Constant at Room Temperature	88
2) Dielectric Constant at Different Temperature	88
4.1.6. Optical Properties	94
1) Transmittance	94
2) Refractive Index	95
4.1.7. Conclusion	99
4.2. The Characterization of Er <sub>2</sub> O <sub>3</sub> Doped KNN-TeO <sub>2</sub> Glass and Glass-ceramic	100
4.2.1. Thermal Behavior Determination	100
4.2.2. Densification Investigation	105
4.2.3. Structural Formation	106
4.2.4. Microstructure Observation	111
4.2.5. Electrical Property	114
4.2.6. Optical Properties	117
1) Absorbance	117
2) Refractive Index and Energy Band Gap	120
3) Photoluminescence	124
4.2.7. Conclusion	125

Chapter 5 Results and Discussion (Part II)	126
Materials Characterization of Potassium Sodium Niobate Based Silicate Glass and Glass-Ceramic	
5.1. The Characterization of KNN-SiO <sub>2</sub> Glass and Glass-Ceramics	126
5.1.1. Thermal Behavior Determination	127
5.1.2. Densification Investigation	129
5.1.3. Structural Formation	130
1) Phase Composition Studied by XRD	130
2) Phase Formation Studied by Raman	130
5.1.4. Microstructural Observation	134
5.1.5. Electrical Property	137
5.1.6. Optical Properties	139
5.1.7. Conclusions	143
5.2. The Characterization of Er <sub>2</sub> O <sub>3</sub> Doped KNN-SiO <sub>2</sub> Glass and Glass-Ceramic	144
5.2.1. Thermal Behavior Determination	144
5.2.2. Densification Investigation	147
5.2.3. Structural Formation	149
1) Phase Composition Studied By XRD	149
2) Phase Formation Studied By Raman	151
5.2.4. Microstructural Observation	152
5.2.5. Electrical Property	155
5.2.6. Optical Properties	156
1) Absorbance	156
2) Photoluminescence spectra	163
5.2.7. Conclusions	166
Chapter 6 Conclusions	167
6.1. General Conclusions	167
6.1.1. KNN-TeO <sub>2</sub> Glasses and Glass-ceramics and Effect of Er <sub>2</sub> O <sub>3</sub> Dopant	167
6.1.2. KNN-SiO <sub>2</sub> Glasses and Glass-ceramics and	168

Effect of Er <sub>2</sub> O <sub>3</sub> Dopant	
6.2. Recommendation for Future Work	172
References	173
List of publications	188
Appendix	189
Appendix A	189
Appendix B	191
Curriculum Vitae	192



ลิขสิทธิ์มหาวิทยาลัยเชียงใหม่  
 Copyright© by Chiang Mai University  
 All rights reserved

## LIST OF TABLES

		Page
Table 2.1	The type of non-polar (non-centrosymmetric) point groups.	8
Table 2.2	List of cations regularly formed perovskite-structured oxides with the ionic radius.	13
Table 2.3	The tolerance factor of some perovskite and their properties.	13
Table 2.4	Electrical property of lead-free systems vs PZT.	19
Table 2.5	Dielectric and piezoelectric properties of lead free KNN based ceramic systems.	19
Table 2.6	The summarized of favorable properties of glass-ceramics.	23
Table 2.7	Optical parameter of $\text{Er}^{3+}$ in various solid host materials.	38
Table 2.8	Density, refractive index, concentration of $\text{Er}^{3+}$ inside glass, glass transition -crystallization temperature and glass stability.	42
Table 3.1	Nominal composition of the starting powders used in this study.	53
Table 3.2	Quantitative analysis of calcined KNN powder at 900 °C for 5 hours by EDS technique.	55
Table 3.3	Chemical compositions of the prepared glass samples.	57
Table 4.1	Thermal profile data of 2 glass compositions from DTA measurement.	78
Table 4.2	The calculated average crystallite sizes in two glass compositions.	83
Table 4.3	Refractive indices of various heat treatment temperature glass-ceramics samples of two glass composition.	99
Table 4.4	Density and thermal profile data of all glass samples.	103

Table 4.5	Summary of crystal morphology and crystallite sizes.	112
Table 4.6	Refractive index and energy band gap of each glass composition.	121
Table 5.1	The thermal profile and glass stability factor of 75KNN-25SiO <sub>2</sub> and 80KNN-20SiO <sub>2</sub> glasses. ( $T_g$ = Glass transition temperature, $T_x = T_c$ onset point, $T_c$ = Crystallization temperature, $\Delta T$ = Glass stability)	128
Table 5.2	Physical properties data of 75KNN-25SiO <sub>2</sub> and 80KNN-20SiO <sub>2</sub> glass systems. (* $L$ , length, $D$ , diagonal values, $d$ , crystallite size)	137
Table 5.3	Refractive index of 75KNN-25SiO <sub>2</sub> and 80KNN-20SiO <sub>2</sub> glass systems.	139
Table 5.4	The stability of glass-ceramics from their DTA thermal profile.	146
Table 5.5	Calculated energy band gap ( $E_g$ ) of the Er <sup>3+</sup> doped KNN-SiO <sub>2</sub> glass-ceramics heat treated at various temperatures.	163
Table 6.1	Comparison of glass transition temperature ( $T_g$ ), crystallization temperature ( $T_c$ ), glass stability factor ( $\Delta T$ ), density ( $\rho$ ), refractive index ( $n$ ), energy band gap ( $E_g$ ) and dielectric constant ( $\epsilon_r$ ) at various frequency for KNN based tellurite glass system with related works.	170
Table 6.2	Comparison of glass transition temperature ( $T_g$ ), crystallization temperature ( $T_c$ ), glass stability factor ( $\Delta T$ ), density ( $\rho$ ), refractive index ( $n$ ), energy band gap ( $E_g$ ) and dielectric constant ( $\epsilon_r$ ) at various frequency for KNN based silicate glass system with related works.	171

## LIST OF FIGURES

	Page
Figure 1.1	AM1.5 terrestrial solar spectrum. 3
Figure 1.2	Energy conversion process presented by energy level diagrams. 4
Figure 2.1	The flow-chart of piezoelectric and subgroups divided by structural symmetry. 9
Figure 2.2	Hysteresis loops and polarization of ferroelectric materials. 11
Figure 2.3	The perovskite crystal structure. 12
Figure 2.4	Binary phase diagram $\text{KNbO}_3\text{-NaNbO}_3$ . 16
Figure 2.5	The transformation of KNN crystal structure at different temperature. Here P stands for the direction of polarization. 17
Figure 2.6	The comparison between KNN based ceramics and others material (a.) dielectric permittivity as a function of Curie temperature, (b) piezoelectric coefficient as a function of temperature. 20
Figure 2.7	Schematic images of (A) glass, (B) crystal, and (C) glass-ceramic. 21
Figure 2.8	Glass-ceramics mechanism after applied heat treatment temperature. (a) Nuclei formation, (b) nuclei growth and (c) crystal structure in glass matrix. 24
Figure 2.9	The comparative illustrate between crystal type structure and amorphous type structure of silicate glass. 25
Figure 2.10	The schematic of glass atoms arrangement with the effect of slow cooling rate and fast cooling rate from liquid glass to atoms structure. 26



Figure 2.11	The volume change of glass and crystal compared with temperature.	28
Figure 2.12	Schematic depiction of rates of nucleation and crystal growth in glass.	30
Figure 2.13	Tellurite glass structure.	35
Figure 2.14	Silicate glass structure.	36
Figure 2.15	The Er <sub>2</sub> O <sub>3</sub> dopants in various applications.	39
Figure 2.16	Energy levels of triple charge RE ions.	40
Figure 2.17	Energy level of Er <sup>3+</sup> ions in Nb <sub>2</sub> O <sub>5</sub> -TeO <sub>2</sub> glass after applied 975 nm and 798 nm excitation source. GSA is ground state absorption, ESA is excited state absorption and ET is energy transfer.	41
Figure 2.18	Thermal profile of 60TeO <sub>2</sub> -20GeO <sub>2</sub> -10Nb <sub>2</sub> O <sub>5</sub> -10K <sub>2</sub> O (6T2G) and 80TeO <sub>2</sub> -10Nb <sub>2</sub> O <sub>5</sub> -10K <sub>2</sub> O (8T0G) with different mol% of Er <sub>2</sub> O <sub>3</sub> . (T <sub>g</sub> =glass transition temperature, T <sub>c1</sub> and T <sub>c2</sub> =crystallization temperature)	43
Figure 2.19	XRD patterns of heat treatment sample. a) glass 8T0G systems with different percent of Er <sub>2</sub> O <sub>3</sub> , b) glass TeO <sub>2</sub> systems with different composition ranging from 30 – 70 mol% TeO <sub>2</sub> .	43
Figure 2.20	SEM micrograph KNbO <sub>3</sub> ceramic with different percent of Er <sup>3+</sup> dopants.	45
Figure 2.21	The effect of annealing temperature on photoluminescence intensity.	45
Figure 2.22	The XRD results of KNN doped with various Er <sub>2</sub> O <sub>3</sub> contents.	46
Figure 2.23	The up-conversion luminescence spectra of KNN ceramics doped with various Er <sub>2</sub> O <sub>3</sub> content.	47
Figure 2.24	Energy level of KNN ceramics doped with Er <sub>2</sub> O <sub>3</sub> .	47
Figure 2.25	FESEM and TEM image of heat-treated glasses at 800°C. (a) and (b) FESEM observed of glass heat treated for 3 h and 50	48

	h,(c) and (d) SAED from TEM of glass heat treated for 50 h and HRTEM image of lattice fringe.	
Figure 2.26	Dielectric constant of as-received glass and heat treated glass.	48
Figure 2.27	Photoluminescence measurement with different excitation source (a) $\lambda_{ex}= 377$ nm and (b) $\lambda_{ex}= 980$ nm.	49
Figure 3.1	The diagram of conventional glass-ceramic method comparing with incorporation method.	51
Figure 3.2	Schematic diagram of powder preparation process.	54
Figure 3.3	X-ray diffraction patterns of KNN with 5 mol% of $\text{Na}_2\text{CO}_3$ and $\text{K}_2\text{CO}_3$ in ratio 1:1 and calcined at $900^\circ\text{C}$ for 5 h. ( $\text{K}_{0.5}\text{Na}_{0.5}\text{NbO}_3$ phase)	54
Figure 3.4	The SEM image of KNN powder obtained cubic crystal sizes 100-200 nm at $900^\circ\text{C}$ for 5 hours.	55
Figure 3.5	Platinum crucible.	56
Figure 3.6	Electric furnace.	57
Figure 3.7	Stainless steel plates.	58
Figure 3.8	Schematic diagram of KNN based $\text{TeO}_2$ glass preparation process.	58
Figure 3.9	Schematic diagram of KNN based $\text{SiO}_2$ glass preparation process.	58
Figure 3.10	Schematic diagram Crystallization process for glass ceramics.	59
Figure 3.11	Differential thermal analyzer, DTA.	60
Figure 3.12	Precision weighing balance.	61
Figure 3.13	X-ray diffractometer.	63
Figure 3.14	Raman spectrometer.	64
Figure 3.15	FTIR spectroscopy operating system.	64
Figure 3.16	SEM-EDS spectroscopy.	65
Figure 3.17	UV-Vis-NIR spectrophotometer.	66
Figure 3.18	Schematic diagram of refraction by light from air to glass to air.	67

Figure 3.19	Refractometer.	69
Figure 3.20	Ellipsometer.	70
Figure 3.21	Fluorescence spectrometer.	72
Figure 3.22	Schematic diagram of fluorescence spectrometer adjustment.	72
Figure 3.23	Coating electrode in irregular shape sample.	73
Figure 3.24	LCZ meter.	73
Figure 4.1	Appearance of as-received glasses (30KNN-70TeO <sub>2</sub> ) melted at various temperatures and times; (a) 1000°C for 15 minutes, (b) 900°C for 15 minutes, (c) 800°C for 15 minutes, (d) 800°C for 30 minutes and (e) 800°C for 60 minutes.	75
Figure 4.2	Thermal analysis (DTA) of KNN-TeO <sub>2</sub> glasses which were melted at 900°C for 15 minutes and quenched between stainless steel plates at room temperature.	76
Figure 4.3	Physical appearances of 30KNN- 70TeO <sub>2</sub> glass-ceramics after various heat treatment (HT) temperatures a) annealed glass at 300°C, b) HT at 325°C, c) HT at 350°C, d) HT at 420°C and e) HT at 522°C.	78
Figure 4.4	Physical appearances of 20KNN- 80TeO <sub>2</sub> glass-ceramics at various heat treatment temperatures (HT) a) annealed glass at 300°C b) HT at 325°C, c) HT at 350°C, d) HT at 408°C and e) HT at 498°C.	79
Figure 4.5	Density of glass and glass-ceramics comparing with HT temperature.	80
Figure 4.6	XRD patterns of two series of glass-ceramics 30KNN-70TeO <sub>2</sub> (a) and 20KNN-80TeO <sub>2</sub> (b) after various HT temperatures. (●=KNbTeO <sub>6</sub> peaks, ⊗ =α-TeO <sub>2</sub> peaks, * =KNN solid solution, ◆=Na <sub>2</sub> Nb <sub>4</sub> O <sub>11</sub> peaks and u=unidentified phases)	81
Figure 4.7	FTIR patterns of 20KNN-80TeO <sub>2</sub> and 30KNN-70TeO <sub>2</sub> systems after heat treatment at T <sub>c1</sub> and T <sub>c2</sub> .	84

Figure 4.8	SEM-EDS of 30KNN- 70TeO <sub>2</sub> glass-ceramics heat treated at different temperatures.	86
Figure 4.9	SEM-EDS of 20KNN- 80TeO <sub>2</sub> glass-ceramics heat treated at different temperatures.	87
Figure 4.10	Dielectric constant (a) and dielectric loss (b) of two series of glass-ceramics at various HT temperatures and frequencies.	89
Figure 4.11	Dielectric constant and loss of glass-ceramics 30KNN-70TeO <sub>2</sub> heat treated at 420°C (T <sub>c1</sub> ) for 4 hours.	90
Figure 4.12	Dielectric constant and loss of glass-ceramics 30KNN-70TeO <sub>2</sub> heat treated at 522°C (T <sub>c2</sub> ) for 4 hours.	91
Figure 4.13	Dielectric constant and loss of glass-ceramics 20KNN-80TeO <sub>2</sub> heat treated at 408°C (T <sub>c1</sub> ) for 4 hours.	92
Figure 4.14	Dielectric constant and loss of glass-ceramics 20KNN-80TeO <sub>2</sub> heat treated at 498°C (T <sub>c2</sub> ) for 4 hours.	93
Figure 4.15	The percent transparent of glass-ceramic which heat treated at various temperatures.	96
Figure 4.16	Refractive index of glass-ceramic which heat treated at various temperatures.	97
Figure 4.17	Photo energy of glass-ceramics 30KNN-70TeO <sub>2</sub> and 20KNN-80TeO <sub>2</sub> .	98
Figure 4.18	Thermal analysis of 30KNN-70TeO <sub>2</sub> glass doped with 0-1 mol% of Er <sub>2</sub> O <sub>3</sub> . (A.-B.) Glass composition of 30KNN-70TeO <sub>2</sub> . (C.-D.) Glass composition of 0.5 mol% Er <sub>2</sub> O <sub>3</sub> doped 30KNN-70TeO <sub>2</sub> . (E.-H.) Glass composition of 1.0 mol% Er <sub>2</sub> O <sub>3</sub> doped 30KNN-70TeO <sub>2</sub> .	102
Figure 4.19	The appearances of glass 30KNN-70TeO <sub>2</sub> doped with Er <sub>2</sub> O <sub>3</sub> of about 0.5 mol% and heat treatment for 4 hours at various temperatures.	104
Figure 4.20	The appearances of glass 30KNN-70TeO <sub>2</sub> doped with Er <sub>2</sub> O <sub>3</sub> of about 1.0 mol% and heat treatment for 4 hours at various temperatures.	104

Figure 4.21	Density of glass ceramics 30KNN-70TeO <sub>2</sub> doped with 0.5 mol% Er <sub>2</sub> O <sub>3</sub> in system C. and D.	105
Figure 4.22	Density of glass ceramics 30KNN-70TeO <sub>2</sub> doped with 1.0 mol% Er <sub>2</sub> O <sub>3</sub> in system E., F., G., and H.	106
Figure 4.23	XRD pattern of glass ceramics 30KNN-70TeO <sub>2</sub> doped with 0.5 mol% Er <sub>2</sub> O <sub>3</sub> in system C. and D. (melted at 800°C for 15min (C.) and 30min (D.), respectively) after heat treatment at various temperature.	108
Figure 4.24	XRD patterns of glass ceramics 30KNN-70TeO <sub>2</sub> doped with 1.0 mol% Er <sub>2</sub> O <sub>3</sub> in system E. and F. (melted at 800°C for 30min (E.) and 60min (F.)) after heat treatment at various temperature.	109
Figure 4.25	XRD patterns of glass ceramics 30KNN-70TeO <sub>2</sub> doped with 1.0 mol% Er <sub>2</sub> O <sub>3</sub> in system G. and H. (melted at 900°C for 30min (G.) and 60min (H.)) after heat treatment at various temperature.	110
Figure 4.26	SEM micrographs of glass ceramics 30KNN-70TeO <sub>2</sub> doped with 0.5 mol% Er <sub>2</sub> O <sub>3</sub> in system C. and D. (melted at 800°C for 15min (C.) and 30min (D.), respectively) after heat treatment at various temperature.	112
Figure 4.27	SEM micrographs of glass ceramics 30KNN-70TeO <sub>2</sub> doped with 1.0 mol% Er <sub>2</sub> O <sub>3</sub> in system E., F., G. and H. (melted at 800°C for 30min (E.) and 60min (F.) and melted at 900°C for 30min (G.) and 60min (H.)) after heat treatment at various temperature.	113
Figure 4.28	Dielectric constants and dielectric losses of glass ceramics 30KNN-70TeO <sub>2</sub> doped with 0.5 mol% Er <sub>2</sub> O <sub>3</sub> in system C. and D. (melted at 800°C for 15min (C.) and 30min (D.), respectively) after heat treatment at various temperature.	114
Figure 4.29	Dielectric constants of glass ceramics 30KNN-70TeO <sub>2</sub> doped with 1.0 mol% Er <sub>2</sub> O <sub>3</sub> in system E., F., G. and H.	115

Figure 4.30	Dielectric losses of glass ceramics 30KNN-70TeO <sub>2</sub> doped with 1.0 mol% Er <sub>2</sub> O <sub>3</sub> in system E., F., G. and H.	116
Figure 4.31	Absorbance spectra of glass ceramics 30KNN-70TeO <sub>2</sub> doped with 0.5 mol% Er <sub>2</sub> O <sub>3</sub> in system C. and D. after heat treatment at different temperatures.	118
Figure 4.32	Absorbance spectra of glass ceramics 30KNN-70TeO <sub>2</sub> doped with 1.0 mol% Er <sub>2</sub> O <sub>3</sub> in system E. and G. after heat treatment at different temperatures.	119
Figure 4.33	The absorption coefficient comparing with heat treatment temperature of 30KNN-70TeO <sub>2</sub> doped 0.5 mol% and 1.0 mol% of Er <sub>2</sub> O <sub>3</sub> .	120
Figure 4.34	Photo energy of glass ceramics 30KNN-70TeO <sub>2</sub> doped with 0.5 mol% Er <sub>2</sub> O <sub>3</sub> in system C. and D. after heat treatment at different temperatures.	122
Figure 4.35	Photo energy of glass ceramics 30KNN-70TeO <sub>2</sub> doped with 1.0 mol% Er <sub>2</sub> O <sub>3</sub> in system E. and G. after heat treatment at different temperatures.	123
Figure 4.36	Photoluminescence patterns of glass 30KNN-70TeO <sub>2</sub> doped with 0.5 mol% Er <sub>2</sub> O <sub>3</sub> samples in system C. and D.	124
Figure 4.37	Photoluminescence patterns of glass 30KNN-70TeO <sub>2</sub> doped with 1.0 mol% Er <sub>2</sub> O <sub>3</sub> in system E. and G.	125
Figure 5.1	The KNN-SiO <sub>2</sub> glass appearances obtained by melted at 1300°C for 15 min.	127
Figure 5.2	DTA traces of the as-quenched glasses from 2 glass series.	128
Figure 5.3	The appearance of glass-ceramics from 2 glass series with different heat treatment temperature. (a.-c. 75KNN-25SiO <sub>2</sub> and d.-f. 80KNN-20SiO <sub>2</sub> )	129
Figure 5.4	The density of 2 glass series varied with heat treatment temperature.	129

Figure 5.5	XRD patterns of glass-ceramic samples at various temperatures. a) 75KNN-25SiO <sub>2</sub> system, b) 80KNN-20SiO <sub>2</sub> system.	132
Figure 5.6	Raman spectra of glass-ceramic samples at various temperatures. a) 75KNN-25SiO <sub>2</sub> system, b) 80KNN-20SiO <sub>2</sub> system.	133
Figure 5.7	SEM micrographs of glass-ceramic samples after heat treatment at various temperatures.	135
Figure 5.8	EDS analysis from SEM micrograph of glass-ceramics 75KNN-25SiO <sub>2</sub> and 80KNN-20SiO <sub>2</sub> which heat treatment at different temperatures.	136
Figure 5.9	The dielectric constant and dielectric loss of 2 glass series heat treated at various temperature.	138
Figure 5.10	Percent transmittance of as-quenched glasses and glass-ceramic samples at various HT temperatures.	140
Figure 5.11	The absorption spectrum of as-quenched glasses and glass-ceramic samples at various HT temperatures.	141
Figure 5.12	The energy band gap values of as-quenched glasses and glass-ceramic samples at various HT temperatures.	142
Figure 5.13	Thermal profile data of all glass samples by using DTA.	145
Figure 5.14	The appearance of glasses and glass-ceramics of 70KNN-30SiO <sub>2</sub> at various heat treatment temperatures. (a) doped 0.5mol% Er <sub>2</sub> O <sub>3</sub> , (b) doped 1.0mol% Er <sub>2</sub> O <sub>3</sub> .	146
Figure 5.15	The appearance of glasses and glass-ceramics of 75KNN-25SiO <sub>2</sub> at various heat treatment temperatures. (a) doped 0.5mol% Er <sub>2</sub> O <sub>3</sub> , (b) doped 1.0mol% Er <sub>2</sub> O <sub>3</sub> .	147
Figure 5.16	The appearance of glasses and glass-ceramics of 80KNN-20SiO <sub>2</sub> at various heat treatment temperatures. (a) doped 0.5mol% Er <sub>2</sub> O <sub>3</sub> , (b) doped 1.0mol% Er <sub>2</sub> O <sub>3</sub> .	147
Figure 5.17	The density of glass ceramics 70KNN-30SiO <sub>2</sub> doped with 0.5 mol% and 1.0 mol% of Er <sub>2</sub> O <sub>3</sub> .	148

Figure 5.18	The density of glass ceramics 75KNN-25SiO <sub>2</sub> doped with 0.5 mol% and 1.0 mol% of Er <sub>2</sub> O <sub>3</sub> .	148
Figure 5.19	The density of glass ceramics 80KNN-20SiO <sub>2</sub> doped with 0.5 mol% and 1.0 mol% of Er <sub>2</sub> O <sub>3</sub> .	149
Figure 5.20	XRD pattern of 70KNN-30SiO <sub>2</sub> and 80KNN-20SiO <sub>2</sub> glass-ceramics doped 0.5-1.0mol% Er <sub>2</sub> O <sub>3</sub> heat treated at various temperatures.	150
Figure 5.21	The raman spectra of 70KNN-30SiO <sub>2</sub> and 80KNN-20SiO <sub>2</sub> doped 0.5 and 1.0 mol% Er <sub>2</sub> O <sub>3</sub> and heat treated at T <sub>g</sub> and T <sub>c</sub> , respectively.	153
Figure 5.22	SEM micrographs of glass-ceramics 70KNN-30SiO <sub>2</sub> doped 0.5-1.0 Er <sub>2</sub> O <sub>3</sub> heat treatment at 550°C (a, d), 600°C (b, e) and 650°C (c, f).	154
Figure 5.23	SEM micrographs of glass-ceramics 80KNN-20SiO <sub>2</sub> doped 0.5-1.0 Er <sub>2</sub> O <sub>3</sub> heat treatment at 500°C (a, d), 550°C (b, e) and 570°C (c, f).	154
Figure 5.24	Dielectric constant and dielectric loss of 2 glass-ceramic conditions after various heat treatment temperatures.	156
Figure 5.25	Absorption spectra of the Er <sup>3+</sup> doped KNN-SiO <sub>2</sub> glass-ceramics heat treated at various temperatures.	158
Figure 5.25	(continue) Absorption spectra of the Er <sup>3+</sup> doped KNN-SiO <sub>2</sub> glass-ceramics heat treated at various temperatures.	159
Figure 5.26	Plots of (ahv) <sup>2</sup> versus hv of the Er <sup>3+</sup> doped 70KNN-30SiO <sub>2</sub> glass-ceramics.	160
Figure 5.27	Plots of (ahv) <sup>2</sup> versus hv of the Er <sup>3+</sup> doped 75KNN-25SiO <sub>2</sub> glass-ceramic.	161
Figure 5.28	Plots of (ahv) <sup>2</sup> versus hv of the Er <sup>3+</sup> doped 80KNN-20SiO <sub>2</sub> glass-ceramics.	162
Figure 5.29	Schematic of glass-ceramics composition.	164
Figure 5.30	Photoluminescence spectra of 75KNN-25SiO <sub>2</sub> doped 0.5mol% Er <sub>2</sub> O <sub>3</sub> and 1.0mol% Er <sub>2</sub> O <sub>3</sub> under 310-415 nm excitation.	165



- Figure 5.31 Photograph of glass ceramics 75KNN-25SiO<sub>2</sub> doped 0.5mol% Er<sub>2</sub>O<sub>3</sub> (1) 0.5HT500, (2) 0.5HT550, (3) 0.5HT600, and 1.0mol% Er<sub>2</sub>O<sub>3</sub> (4) 1.0HT500, (5) 1.0HT550 (6) 1.0HT600 luminescence under 310-415 nm excitation. 165
- Figure 5.32 Energy level diagram of Er<sup>3+</sup> ions with luminescence mechanism. 166



ลิขสิทธิ์มหาวิทยาลัยเชียงใหม่  
Copyright© by Chiang Mai University  
All rights reserved

## LIST OF ABBREVIATIONS

ASTM	American Standard Testing of Materials
a.u.	Arbitrary Unit
BT	Barium Titanate
cm	Centimeter
°C	Degree Celcius
CIP	Cold Isostatic Pressure
DTA	Differential Thermal Analysis
E	Electric Field
E <sub>c</sub>	Coercive Field
E <sub>g</sub>	Energy Gap
eV	Electron Volt
EDS	Energy Dispersive Spectroscopy
FE	Ferroelectric
FESEM	Field Emission Scanning Electron Microscopy
FTIR	Fourier Transform Infrared Spectroscopy
FWHM	Full-Width at Half Maximum
g	Grams
GHz	Gigahertz
h	Hour
h	Planck's Constant
HP	Hot Isostatic Pressure
HT	Heat treatment
Hz	Hertz
IR	Infrared
JCPDS	Joint Committee on Powder Diffraction Standards
KN	Potassium Niobate
KNN	Potassium Sodium Niobate
kHz	Kilohertz

$k_p$	Coupling Factor Coefficient
LN	Lanthanide
LN	Lithium Niobate
m	Meter
mm	Millimeter
$\mu\text{m}$	Micrometer
MHz	Megahertz
Mol%	Percent by Mol
MPB	Morphotopic Phase Boundary
n	Refractive Index
NIR	Near-Infrared
NLO	Non-Linear Optical
nm	Nanometer
NN	Sodium Niobate
P	Polarization
$P_s$	Spontaneous Polarization
$P_r$	Remnant Polarization
pC/N	Picocoulomb per Newton
PL	Photoluminescence
PLZT	Lead Zirconate Titanate
PMN	Lead Manganese Niobate
PT	Lead Titanate
PZT	Lead Zirconate Titanate
RE	Rare Earth
s	Second minuet
SHG	Second Harmonic Generation
$T_C$	Curie Temperature
$T_c$	Crystallization Temperature
$T_g$	Glass Transition Temperature
$T_x$	Onset of Crystallization Temperature
$T_m$	Melting Temperature
TFGC	Transparent Ferroelectric Glass-ceramics

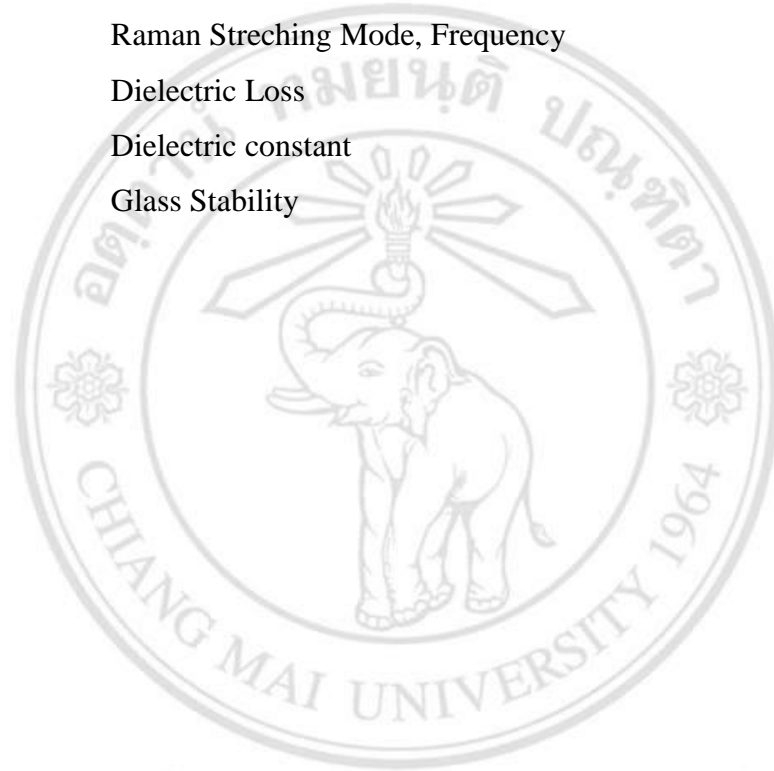
TGG	Template Grain Growth
UV	Ultraviolet
VIS	Visible
Wt%	Percent by Weight
XRD	X-ray Diffractometer



ลิขสิทธิ์มหาวิทยาลัยเชียงใหม่  
Copyright© by Chiang Mai University  
All rights reserved

## LIST OF SYMBOLS

$\alpha$	Alpha, Absorption Coefficient
$\lambda$	Lambda, Wavelength
$\theta$	Theta, Degree
$\nu$	Raman Stretching Mode, Frequency
$\tan\delta$	Dielectric Loss
$\epsilon_r$	Dielectric constant
$\Delta T$	Glass Stability



ลิขสิทธิ์มหาวิทยาลัยเชียงใหม่  
Copyright© by Chiang Mai University  
All rights reserved

## ข้อความแห่งการริเริ่ม

- 1) งานวิจัยนี้ได้นำเสนอแก้วเซรามิกระบบใหม่จากสารเฟอร์โรอิเล็กทริกโพแทสเซียมโซเดียมไนโอเบตที่เจือแร่หายากชนิดเออร์เบียมไดออกไซด์ เพื่อให้ได้แก้วเซรามิกที่มีคุณสมบัติไฟฟ้าเชิงแสงที่นำไปประยุกต์ใช้เป็นซับสเตรตโปร่งแสงและสามารถเพิ่มประสิทธิภาพเซลล์แสงอาทิตย์ได้
- 2) นอกจากนี้ในงานวิจัย ยังได้นำเสนอวิธีการปรับปรุงการเตรียมแก้วเซรามิกที่เรียกว่าวิธีอินคอร์ปอเรชันในขั้นตอนก่อนการหลอมแก้ว เนื่องจากเป็นที่ทราบกันดีว่ากระบวนการเตรียมแก้วเซรามิกมักประสบปัญหาการผ่นผวนขององค์ประกอบของสารตัวเติมในระหว่างกระบวนการหลอมเสมอ ทำให้งานนี้สามารถปรับปรุงแก้วเซรามิกให้มีองค์ประกอบที่ต้องการได้

ลิขสิทธิ์มหาวิทยาลัยเชียงใหม่  
Copyright© by Chiang Mai University  
All rights reserved

## STATEMENT OF ORIGINALITY

- 1) This dissertation represent the new system of ferroelectric glass-ceramic potassium sodium niobate with erbium dioxide rare earth dopants, in order to increase electro-optic property for transparent substrate, lead to the increase of solar cell efficiency.
- 2) In addition, this research also offers an alternative method as the incorporation method in glass-melting step. It is well known that in glass melting step always suffered from composition fluctuation of additives during melting at high temperature. Hence, the incorporation method is useful for create glass-ceramics with desired phase composition.



ลิขสิทธิ์มหาวิทยาลัยเชียงใหม่  
Copyright© by Chiang Mai University  
All rights reserved